COMPARISON OF THE PERFORMANCE OF MEDIUM AND LOW LEVEL GNSS APPARATUS, WITH AND WITHOUT REFERENCE NETWORKS

M. A. Brovelli [a], E. Realini [a]*, M. Reguzzoni [a], M. G. Visconti [a]

[a] DIIAR, Politecnico di Milano, Polo Regionale di Como, via Valleggio 11 Como 22100, Italy – eugenio.realini@polimi.it

KEY WORDS: Mobile mapping, GNSS reference networks, low level GNSS receivers, Real Time Kinematic

ABSTRACT:

The principle of mobile mapping is to combine some surveying techniques with results coming from a navigation apparatus. In this context there is a tendency to try to use cheaper and simpler devices, particularly for GNSS receivers. At the same time there is an increasing diffusion of reference networks of permanent GNSS stations. In this paper we investigate to what extent the differential positioning can alleviate the degradation of accuracy due to the use of medium and low level devices.
Some experiments of RTK and kinematic positioning elaborated with and without corrections coming from permanent GNSS stations are described. It turns out that differential corrections significantly enhance the information acquired by medium level GNSS devices, although in some cases also stand-alone low level apparatus can have performances of unexpected good accuracy.

1. INTRODUCTION

Mobile mapping systems are usually composed by various apparatus, among which there are those providing position, velocity and attitude of the mobile device at every epoch (Sansò, 2006). In this work we focus on GNSS positioning systems (Hofmann-Wellenhof et al., 2001), and in particular on the performances of medium and low level GNSS devices, which are solutions mostly adopted for navigation purposes. These devices usually use C/A code and L1 frequency, and they are expected to provide a positioning accuracy of some meters. For most mobile mapping applications this accuracy can be acceptable, but for specific applications such as, for example, the monitoring of trucks carrying hazardous substances, better accuracy levels are required.
One way to improve GNSS positioning is the use of GNSS reference networks (Biagi et al., 2006), which provide corrections for GNSS measurements, allowing an improvement of positioning accuracies.
The aim of this work is to evaluate the intrinsic accuracy of low and medium level GNSS receivers and the potential improvement provided by the use of differential corrections coming from a regional network of permanent GNSS stations. To achieve this, various tests along straight and curved paths have been performed, in order to evaluate the receivers behaviour under different conditions that are representative of normal vehicle movements.
Furthermore, it is known that GNSS chipsets with navigational purposes make use of Kalman filtering; however the software is usually proprietary. In order to investigate this resident software we have implemented two possible Kalman filtering models. They have been conceived so that one is able to better model straight paths, while the other is more capable of modeling curved paths.
Therefore, in order to test the hypothesis that one or the other is in fact implemented into the receivers, different experiments involving both straight and curved trajectories have been performed, comparing results from high, medium and low level GNSS devices.

2. METHODOLOGY

2.1 GNSS devices

All the experiments were carried out using at least one GNSS receiver for each quality class (high, medium and low – characteristics summarized in Table 1). The high level receiver has been used in order to have a reference trajectory to evaluate the errors of the medium and low level receivers.

Receiver	Antenna / GNSS chip	Signals	Channels	Accuracy
Leica GPS1200	Leica ATX1230	L1 / L2 C/A	12 L1 + 12 L2 + 2 SBAS	10 mm + 1 ppm (RTK)
Leica GS20	Leica AT501	L1 C/A	12	40 cm (DGPS)
eBonTek eGPS 248	NEMERIX	L1 C/A	16	3 m (stand-alone)
eBonTek eGPS 597	Atmel ANTARIS 4	L1 C/A	16	2.5 m (stand-alone)
TomTom	SiRF Star III	L1 C/A	20	5 m (stand-alone)

Table 1. GNSS receivers

The high level receiver (Leica GPS1200) has been used in relative RTK (Real-Time Kinematic) positioning with respect to Lombardia GNSS reference network, using VRS (Virtual Reference Station) corrections (see paragraph 2.2).
Since the medium level receiver (Leica GS20) can use code differential corrections (DGPS), it was employed both in absolute and relative positioning, in order to assess the improvements provided by the reference network.
The low level receivers (eBonTek eGPS 248, eBonTek eGPS 597 and TomTom) were used only in absolute (stand-alone) positioning, as they are not able to use any kind of differential correction.

* Corresponding author.

The experiments were carried out during three days: two in kinematic mode and one in static mode, as summarized in Table 2.

Day	Test mode	Receivers
31st of January	kinematic	Leica GPS1200 Leica GS20 eBonTek eGPS 248 TomTom
14th of February	static	eBonTek 248 eBonTek 597
8th of March	kinematic	Leica GPS1200 Leica GS20 eBonTek eGPS 597

Table 2. Experiments

For the kinematic tests, a trolley has been used to move the instrumentation under controlled conditions (Figure 1): the GNSS receivers were positioned on an axis oriented along the direction of movement of the trolley, and the distances between the reference receiver and each of the other receivers were measured (see Table 3).

Day	Receivers	Distance [m]
31st of January	GPS1200 – eGPS248	0.50
	GPS1200 – GS20	0.77
8th of March	GPS1200 – eGPS597	0.36
	GPS1200 – GS20	0.74

Table 3. Distances among receivers

Since the TomTom receiver requires a minimum velocity to assume to be in motion, we discarded it, as otherwise we had to move the trolley too fast.

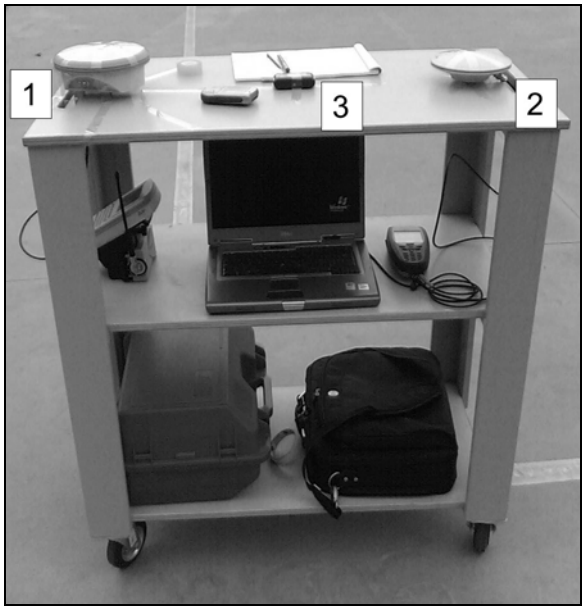

Figure 1. GNSS apparatus configuration for kinematic tests (1: GPS1200, 2: GS20, 3: eGPS 248/597)

The high level receiver had been configured in order to give a text file in output containing the coordinates acquired in real-time at every epoch; the medium level receiver has been connected to a laptop via RS232 serial port, to store the acquired coordinates in NMEA 0183 format in a text file (via VisualGPS software). Besides, in order to allow the GS20 to get the differential corrections (sent over the Internet), a Bluetooth connection was set up between it and a NOKIA 6630 mobile phone, acting as a GPRS modem. The low level receiver was connected via Bluetooth to another NOKIA 6630 mobile phone, with the nTripper software installed, which allowed to acquire and store in text file the coordinates in NMEA 0183 format.

2.2 Lombardia positioning service

Since 2003 a GNSS reference network for positioning services exists in Lombardia region (Biagi and Sansò, 2006). It consists of 17 permanent GNSS stations, homogeneously distributed, covering almost all the region. The services offered by the network can be used for both post-processing and real-time positioning: as for the latter, the available services are essentially aimed to both navigation with metric precision, by means of the distribution of code observations differences (DGPS) (Hofmann-Wellenhof et al., 2003), and real-time static measurements, by means of a network approach with the computation and distribution of carrier phase corrections. Network approaches are based on sending to the rover receiver a function modeling the errors contained in double differences carrier phase; in this paper a VRS approach has been used.

2.3 Kalman filtering simulations

The performance of Kalman filtering has been tested on the basis of two different dynamical models, assuming, apart from noises, either a motion with constant velocity (model A) or with constant acceleration (model B). The former is expected to better predict the trajectory when the motion is along a straight line, while the latter should work better in case of a winding path.

Model A: constant velocity

A motion with a constant velocity is ruled by the following law:

$$\begin{cases} \vec{x}(t) = \vec{v}t + \vec{x}_0 \\ \vec{v} = \text{const} \end{cases} \quad (1)$$

where $\vec{x}(t)$ is the position of the body at time t, $\vec{x}_0$ is the starting position of the system and $\vec{v}$ the constant velocity. Considering a discrete system with a sampling rate of 1 second, the dynamical model becomes

$$\begin{cases} \vec{x}_{t+1} = \vec{v}_t + \vec{x}_t \\ \vec{v}_{t+1} = \vec{v}_t \end{cases} \quad (2)$$

Given the initial state $(\vec{x}_0, \vec{v}_0)$ (which however has to be modelled as a random variable), positions and velocities at every time are strictly determined by this dynamical model. In order to introduce a suitable level of flexibility, it is assumed that the velocity can slightly change from one epoch to another. This is obtained by adding, epoch by epoch, a white noise to the velocity.
All in all, the dynamics of the system can be written as follows

$$\begin{cases} \vec{x}_{t+1} = \vec{v}_t + \vec{x}_t \\ \vec{v}_{t+1} = \vec{v}_t + \vec{\varepsilon}_{t+1} \end{cases} \quad (3)$$

or equivalently

$$\vec{x}_{t+2} - 2\vec{x}_{t+1} + \vec{x}_t = \vec{\varepsilon}_{t+1} \tag{4}$$

Model B: constant acceleration

Repeating the same reasoning of the previous model, but assuming now that the acceleration $\vec{a}$ is constant, apart from an added white noise, the system dynamics can be modelled as follows

$$\begin{cases} \vec{x}_{t+1} = \vec{x}_t + \vec{v}_t \\ \vec{v}_{t+1} = \vec{v}_t + \vec{a}_t \\ \vec{a}_{t+1} = \vec{a}_t + \vec{\varepsilon}_{t+1} \end{cases} \tag{5}$$

Equivalently one could write

$$\vec{x}_{t+3} - 3\vec{x}_{t+2} + 3\vec{x}_{t+1} - \vec{x}_t = \vec{\varepsilon}_{t+1} \tag{6}$$

Simulations

In this paragraph we describe some numerical simulations implemented in MATLAB (Grewal and Andrews, 2001).
At first we have simulated a body moving along a circular trajectory with a radius R=20 m and a constant angular velocity ω=0.05 rad/s. This means that in 200 seconds (observation time) the body covers about 3 laps of the circuit. The noise of the position observations has been given a standard deviation of 0.5 m (Figure 2). In the case of model A the error added to the velocity (system error) had a standard deviation of 0.01 m/s, while in the case of model B the error added to the acceleration had a standard deviation of 0.01 m/s^2.
In this case, after a transition time due to the fact that the starting point is not on the circular path, the Kalman filter based on the model B is able to follow the curvilinear trajectory, while the solution with the model A is too rigid, predicting a circular trajectory with a larger radius (Figure 3). This results in a position error with a systematic bias. The rms error (root mean square error) for the model A is of the order of 5 m against a rms error of 0.2 m for the model B.

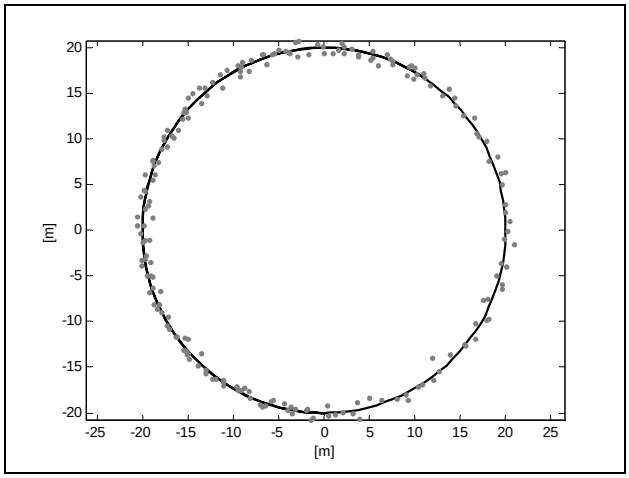

Figure 2. Ideal trajectory (in black) and position observations (in grey) at sampling rate of 1 sec

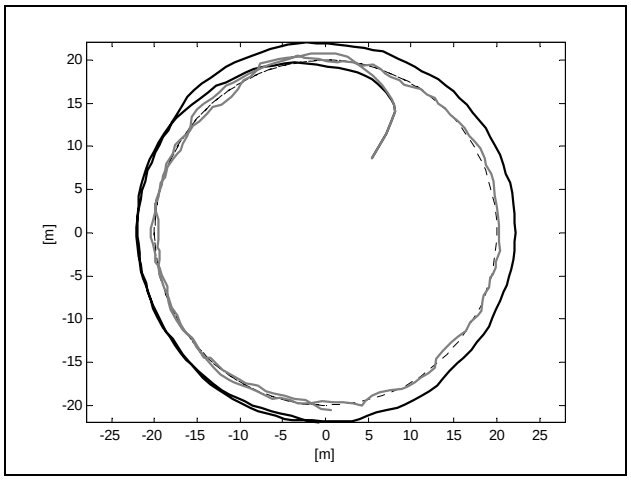

Figure 3. Estimated trajectory using a Kalman filter with the dynamical model A (in black, solid line) and the dynamical model B (in grey, solid line). True trajectory in black dash line

Let us suppose now that the body is moving along the path shown in Figure 4. The observation noise has again a standard deviation of 0.5 m. In the case of model A the velocity error had a standard deviation of 0.005 m/s, while in the case of model B the acceleration error had a standard deviation of 0.005 m/s^2.
This example emphasizes the pros and cons of the two models (Figure 5). In the straight stretches the solution A is more regular, but in the curvilinear sections it runs away from the true path; it needs some additional time to correct the trajectory when the road returns to be straight. On the other hand, the solution B is more wiggling everywhere, but it is capable to follow the true trajectory even in the curvilinear sections.
As a consequence, after the initial transition time, the error level become stable in the case of model B, while it oscillates in the case of model A, depending on the fact that the body is covering a straight or a curvilinear section (note that two of the four straight lines are not long enough to allow the body to come back on the right trajectory). The error rms for the model A is 1.2 m, while for the model B it is about 0.2 m.

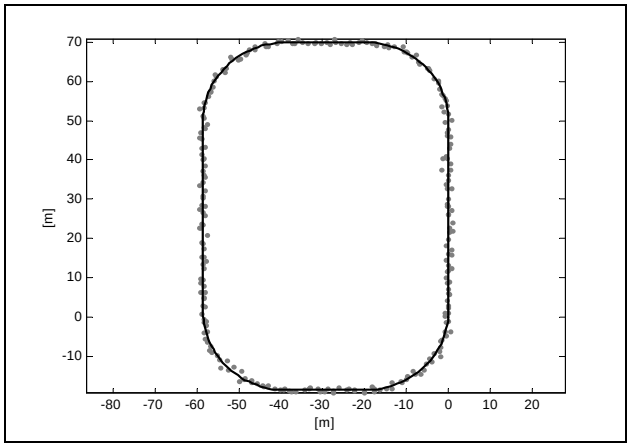

Figure 4. Ideal trajectory (in black) and position observations (in grey) at sampling rate of 1 sec

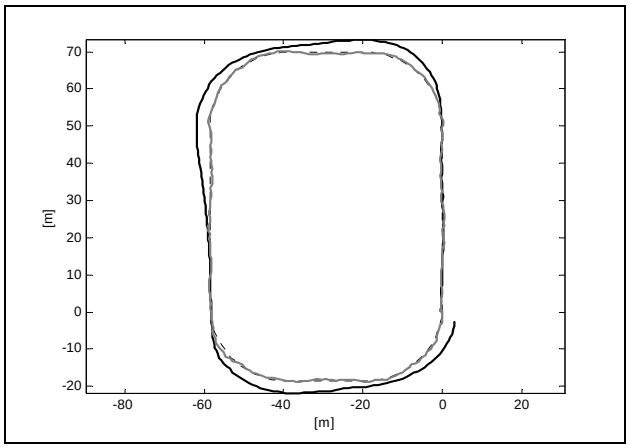

Figure 5. Estimated trajectory using a Kalman filter with the dynamical model A (in black, solid line) and the dynamical model B (in grey, solid line). True trajectory in black dash line

The previous case is repeated along the same path and with the same observations, but now the error added to the velocity in the model A has a standard deviation of 0.05 m/s. In other words, higher model errors are accepted. The corresponding solution becomes much more reactive, following every change of direction. On the other hand, the main advantage of model A is definitively lost, since the trajectory has the same regularity of the one computed by using the model B. Therefore the two solutions are very similar (Figure 6), both with an error rms of 0.2 m.

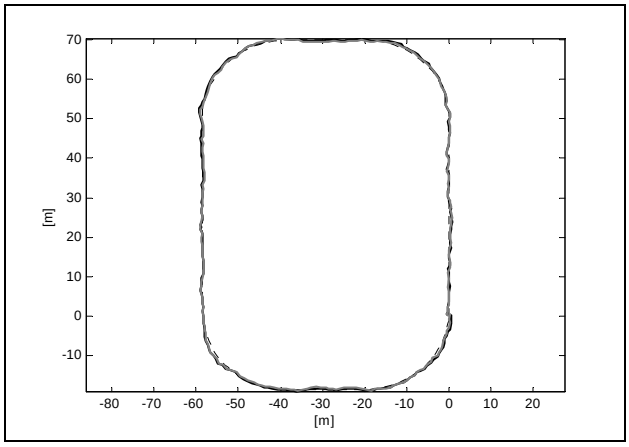

Figure 6. Estimated trajectory using a Kalman filter with the dynamical model A (in black, solid line) and the dynamical model B (in grey, solid line). True trajectory in black dash line

Finally we have simulated a body standing at the same location. Its position is measured every second with an observation noise of 0.5 m (Figure 7). When Kalman filtering is applied, the estimated position however changes in time and the resulting trajectory strays around the true location both in the case of model A and of model B (Figure 8). Note that, due to the randomness of the initial state, the estimated trajectory can start far from the true position and even move in the wrong direction; however, after a transition time, it tends to come back and cluster around the true location.

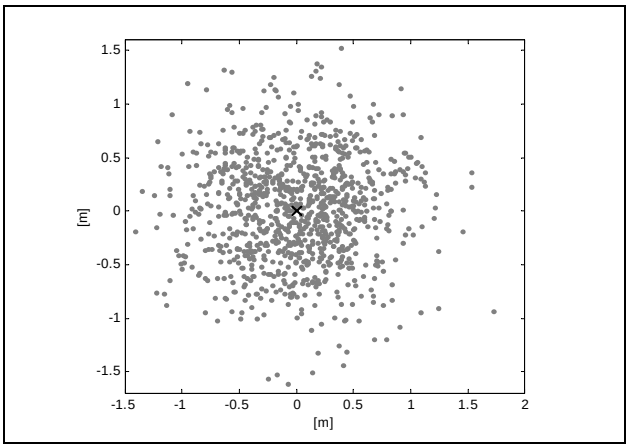

Figure 7. Body location (black cross) and position observations (in grey) at sampling rate of 1 sec

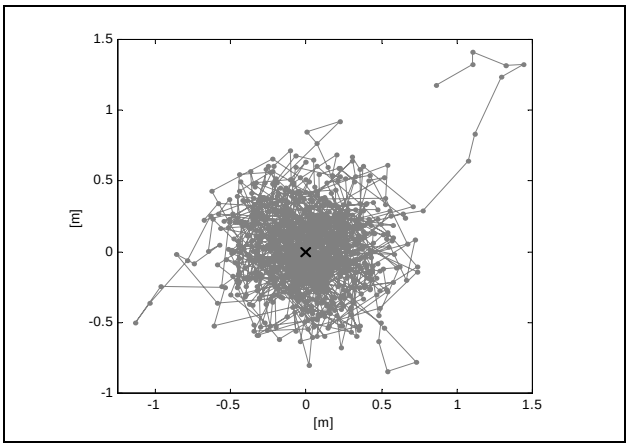

Figure 8. Estimated trajectory using a Kalman filter. The black cross indicates the true position of the body

3. ANALYSIS AND RESULTS

In this paragraph we describe real experiments as mentioned in paragraph 1.

3.1 Data analysis

The experiments are detailed in the following list:

1. 31st of January 2007
    a. path composed by 4 straight lines with angles of 90° using GS20 and eGPS 248 receivers in stand-alone mode;
    b. path composed by 4 straight lines with angles of 90° using GS20 receiver in relative DGPS mode and eGPS 248 receiver in stand-alone mode.

2. 14th of February 2007
    a. around 4 hours of static tests using eGPS 248 and eGPS 597 receivers in stand-alone mode.

3. 8th of March 2007
    a. path composed by 4 straight lines with angles of 90° using GS20 and eGPS 597 receivers in stand-alone mode;

b. path composed by straight lines and curves using GS20 and eGPS 597 receivers in stand-alone mode;
c. circular path using GS20 and eGPS 597 receivers in stand-alone mode.

The coordinates acquired during the kinematic tests by the high level receiver (reference receiver) at every epoch t_0 were interpolated by a four degree polynomial

$$E_{ref}(t_i) = a_1 + b_1 t_i + c_1 t_i^{\,2} + d_1 t_i^{\,3} + e_1 t_i^{\,4}$$
$$N_{ref}(t_i) = a_2 + b_2 t_i + c_2 t_i^{\,2} + d_2 t_i^{\,3} + e_2 t_i^{\,4} \quad (7)$$

using observations over five subsequent epochs, centered on t_0 ($t_{-2}, t_{-1}, t_0, t_{+1}, t_{+2}$). In this way, we estimated the trolley trajectory, and therefore its attitude, since it was moving on a horizontal plane. The choice of four degree polynomials has been based on empirical tests.
Once the coefficients have been determined, calling *b* the time derivative of the position vector ($b_1 = \frac{dE}{dt} = \dot{E}$, $b_2 = \frac{dN}{dt} = \dot{N}$), the unit vector at each point of the trajectory was calculated

$$\vec{e}(t_0) = \frac{1}{\sqrt{(\dot{E}^2 + \dot{N}^2)}} \begin{bmatrix} \dot{E} \\ \dot{N} \end{bmatrix} \quad (8)$$

determining the direction of movement of the trolley on the horizontal plane at every epoch t_0. Knowing $\vec{e}(t_0)$, it has been possible to translate the medium and low level receivers (test receivers) positions to the position of the reference receiver. After that, we calculated the residual $\delta\vec{X}(t_0)$ between the reference coordinates and those of each test receiver at the same epoch t_0 using

$$\hat{\vec{X}}_{test}(t_0) = \vec{X}_{test}(t_0) + D\vec{e}(t_0)$$
$$\delta\vec{X}(t_0) = \hat{\vec{X}}_{test}(t_0) - \vec{X}_{ref}(t_0) \quad (9)$$

where D is the distance between the reference receiver and each test receiver. The computation has been implemented in MATLAB.

3.2 Results

The data obtained by using the different receivers were plotted together with those of the reference receiver (Figures 7-17) and the mean, rms, maximum and minimum values of the differences $\delta\vec{X}$ were computed (Tables 4-13).

31st of January 2007

On this day, two kinds of tests were carried out. The GS20 and eGPS 248 were initially used without differential corrections, then the corrections were applied to the GS20 only, in order to compare its performances with and without reference networks.

GS20 and eGPS 248 in stand-alone mode

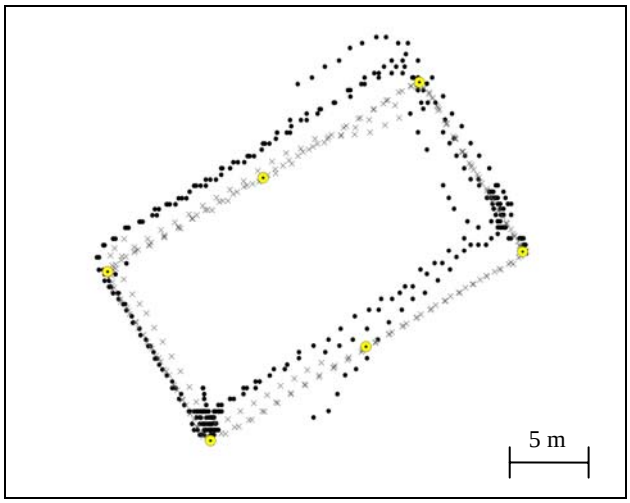

Figure 9. Reference data (grey crosses) and GS20 data (black dots) in stand-alone mode

GS20	*North [m]*	*East [m]*
mean	-1.620	0.999
rms	1.033	0.661
max	2.283	3.816
min	-4.048	-1.956

Table 4. GS20 statistics (stand-alone mode)

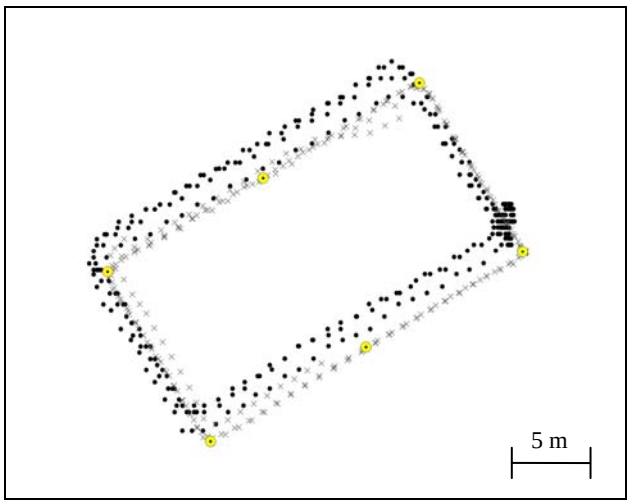

Figure 10. Reference data (grey crosses) and eGPS 248 data (black dots) in stand-alone mode

eGPS 248	*North [m]*	*East [m]*
mean	-1.151	1.359
rms	0.917	0.410
max	1.159	2.0939
min	-2.742	0.655

Table 5. eGPS 248 statistics (stand-alone mode)

The stand-alone behaviours for the two receivers are substantially comparable, even though the GS20 had problems in keeping a straight trajectory.

GS20 in DGPS mode and eGPS 248 in stand-alone mode

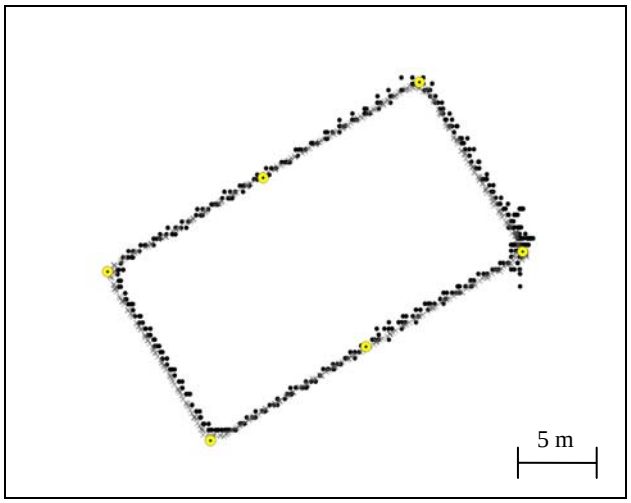

Figure 11. Reference data (grey crosses) and GS20 data (black dots) in DGPS mode

GS20	*North [m]*	*East [m]*
mean	-0.289	-0.206
rms	0.249	0.216
max	0.620	0.959
min	-1.587	-0.804

Table 6. GS20 statistics (DGPS mode)

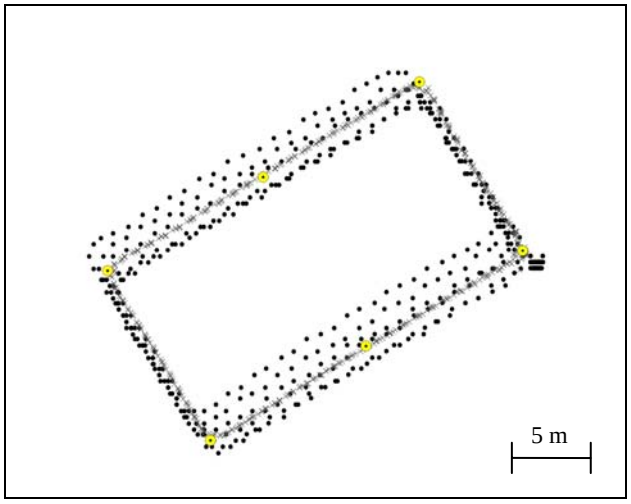

Figure 12. Reference data (grey crosses) and eGPS 248 data (black dots) in stand-alone mode

eGPS 248	*North [m]*	*East [m]*
mean	0.067	0.484
rms	1.128	0.877
max	2.250	2.348
min	-2.502	-1.254

Table 7. eGPS 248 statistics (stand-alone mode)

In this case the GS20 in DGPS mode clearly shows a higher level of accuracy (around 20 cm) and a path that is similar to the one of reference receiver. The eGPS 248 confirms its previous performance.

14th of February 2007

In this experiment we compared the two eBonTek receivers in static mode for a session of about 4 hours. The main purpose of this test was to check if the Kalman filtering models implemented in the two receivers were different, since they had shown very different behaviours during past tests, despite their nominal accuracies being practically the same.

Static tests with eGPS 248 / 597 in stand-alone mode

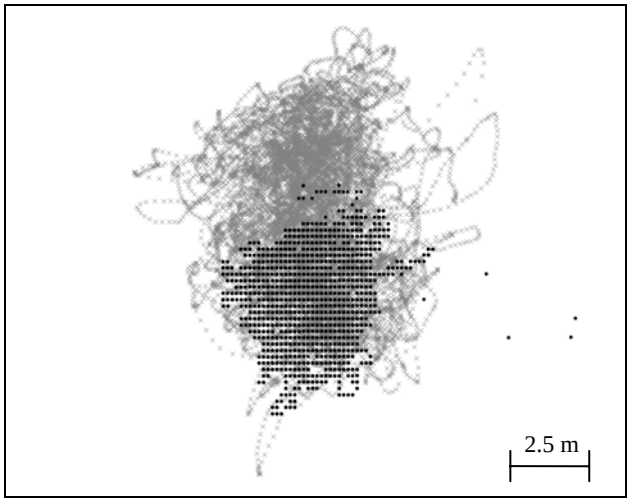

Figure 13. eGPS 597 data (grey crosses) and eGPS 248 data (black dots) in stand-alone static mode

The radius of the two data-sets is quite different (around 5 m for the eGPS 248 and 7-10 m for the eGPS 597) and the eGPS 597 shows a less compact cluster of points (Figure 13). Note that these results are consistent with those coming from the Kalman filtering model in the static case (Figure 8).

8th of March 2007

The tests that were carried out on this third day were mainly aimed at analyzing the behaviours of the devices when following different paths, both straight ones and curved ones.
Since in the tests of the first day the GS20 and eGPS 248 showed very similar behaviours, we decided to use the GS20 as representative of both of them.

Path composed by 4 straight lines with angles of 90°

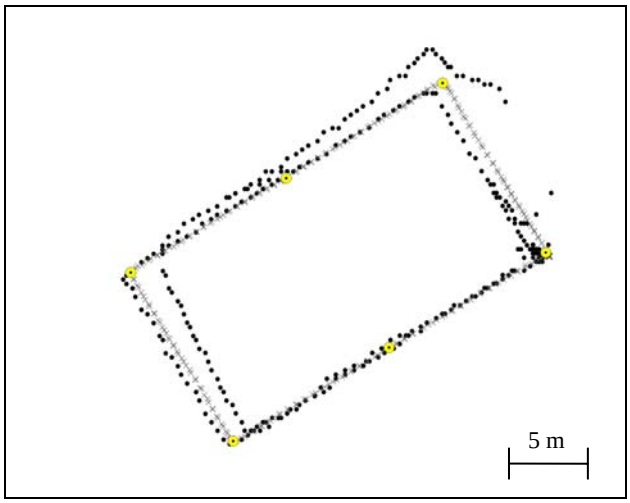

Figure 14. Reference data (grey crosses) and GS20 data (black dots) in stand-alone mode

GS20	*North [m]*	*East [m]*
mean	-0.464	0.185
rms	1.097	1.059
max	0.966	1.856
min	-5.744	-4.746

Table 8. GS20 statistics (stand-alone mode)

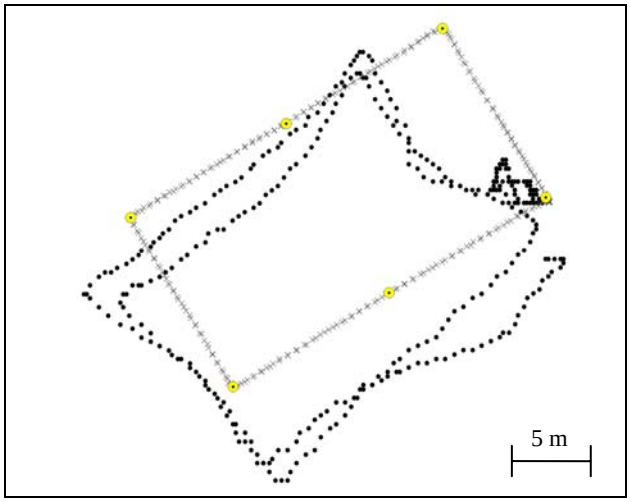

Figure 15. Reference data (grey crosses) and eGPS 597 data (black dots) in stand-alone mode

eGPS 597	*North [m]*	*East [m]*
mean	3.187	1.461
rms	2.748	2.507
max	6.897	5.805
min	-2.998	-3.222

Table 9. eGPS 597 statistics (stand-alone mode)

When following straight trajectories with sudden changes of direction, the GS20 confirmed the previous tests (without differential corrections), while the eGPS 597 behaved very differently (Figure 13). Its reaction to the sudden changes of direction was in fact slow, causing a path deformation, similar to the trajectory computed with model A (Figure 5), apart from a shift in the south-west direction (probably due to the different satellite selection algorithms).

Path composed by straight lines and curves

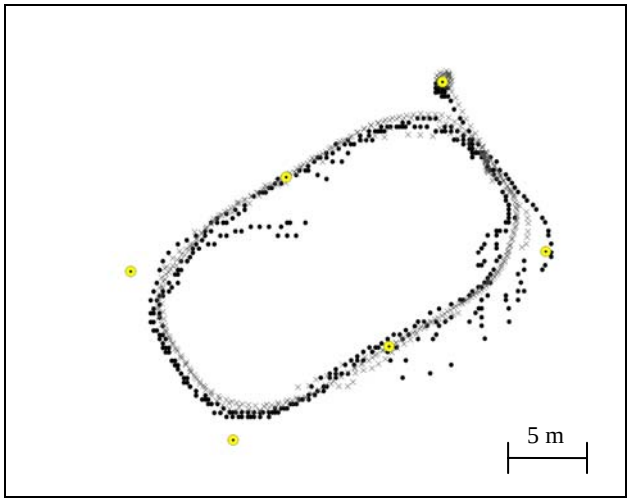

Figure 16. Reference data (grey crosses) and GS20 data (black dots) in stand-alone mode

GS20	*North [m]*	*East [m]*
mean	0.589	0.246
rms	0.716	0.745
max	4.529	2.003
min	-2.774	-2.653

Table 10. GS20 statistics (stand-alone mode)

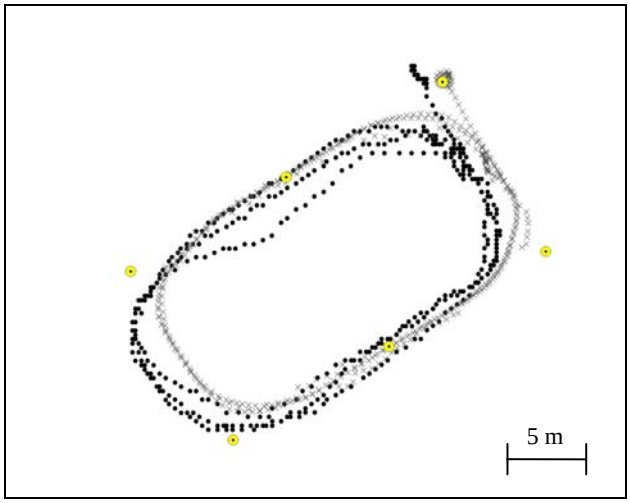

Figure 17. Reference data (grey crosses) and eGPS 597 data (black dots) in stand-alone mode

eGPS 597	*North [m]*	*East [m]*
mean	0.648	1.635
rms	0.976	0.764
max	3.631	4.509
min	-3.023	-0.294

Table 11. eGPS 597 statistics (stand-alone mode)

When following a path with smooth changes of direction, the two receivers give very similar results, both in terms of trajectory and statistics.

Circular path

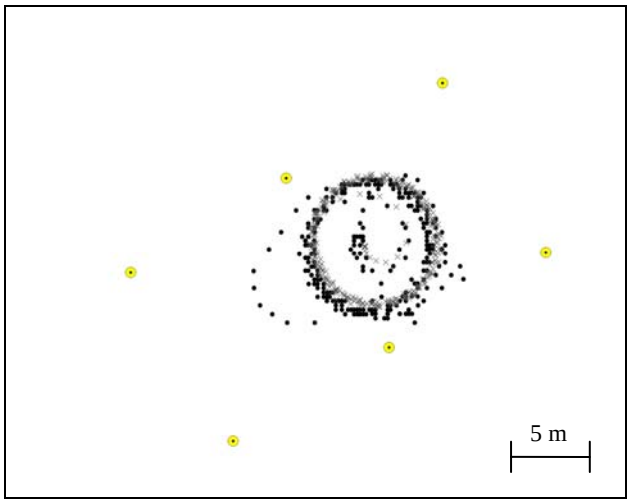

Figure 18. Reference data (grey crosses) and GS20 data (black dots) in stand-alone mode

GS20	*North [m]*	*East [m]*
mean	0.480	0.298
rms	0.317	1.217
max	1.320	5.511
min	-1.110	-3.346

Table 12. GS20 statistics (stand-alone mode)

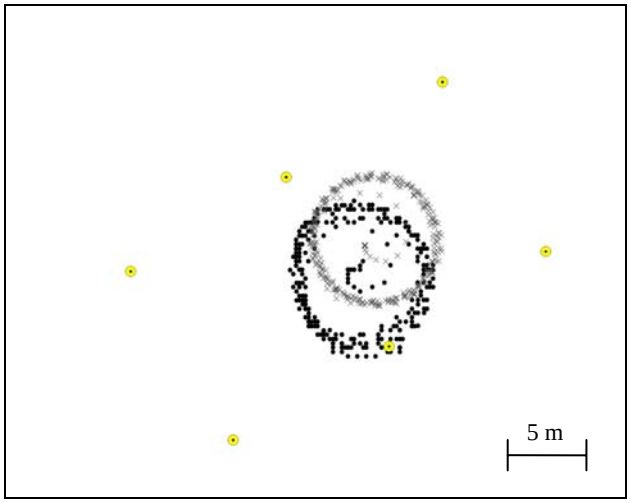

Figure 19. Reference data (grey crosses) and eGPS 597 data (black dots) in stand-alone mode

eGPS 597	*North [m]*	*East [m]*
mean	2.575	1.028
rms	0.705	0.563
max	4.356	2.407
min	1.289	-0.118

Table 13. eGPS 597 statistics (stand-alone mode)

When following a circular path the GS20 tends to stay close to the reference circle, while the data collected by the eGPS 597 show, as in the previous cases, a shift to the south-west and a radius slightly larger than the one of the reference data; this is similar to the behaviour of the model A along a circular trajectory (Figure 3).

4. CONCLUSION

The tests have shown that medium and low level receivers, such as for example the Leica GS20 and the eBonTek 248/597 have very similar behaviours; trajectories are systematically shifted and errors are comparable.
On the other hand, using differential corrections the Leica GS20 receiver shows a behaviour that could be substantially compared to the high level receiver.
Table 14 summarizes the precision achievable with the medium and low level apparatus.

Receiver	**DGPS**	**rms [m]**
eBonTek	No	~ 1
Leica GS20	No	~ 1
Leica GS20	Yes	~ 0.2

Table 14. medium and low level apparatus statistics

As regards the Kalman filtering models, the constant acceleration hypothesis (Model B) seems to be confirmed for the eBonTek 248 and Leica GS20 receivers, while the eBonTek 597 has a behaviour suggesting that a constant velocity hypothesis (Model A) for its dynamics has been implemented.

5. REFERENCES

Biagi, L., Crespi, M., Manzino, A., Sansò, F., 2006. I servizi di posizionamento basati su reti di stazioni permanenti GNSS. In: *Bollettino SIFET*, 1, pp. 29-59.

Biagi, L., Sansò, F., et al., 2006. Il servizio di posizionamento in Regione Lombardia e la prima sperimentazione sui servizi di rete in tempo reale. In: *Bollettino SIFET*, 3, pp. 71-90.

Grewal, M. S. and Andrews, A. P., 2001. *Kalman Filtering, Theory and Practice Using MATLAB*. Wiley and sons, New York.

Hofmann-Wellenhof, B., Lichtenegger, H. and Collins, J., 2001. *GPS – Theory and Practice*. Springer-Verlag Wien, New York.

Hofmann-Wellenhof, B., Legat, K., Wieser, M., 2003. *Navigation, Principles of Positioning and Guidance*. Springer-Verlag Wien, New York.

Sansò, F., 2006. *Navigazione geodetica e rilevamento cinematico*. Polipress, Milano.